Enhancing natural killer cell function with gp41-targeting bispecific antibodies to combat HIV infection

Nitya S. Ramadoss[a,f,*], Nancy Q. Zhao[b,c,*], Barbra A. Richardson[d], Philip M. Grant[b], Peter S. Kim[a,e,f] and Catherine A. Blish[b,c,e]

Objective(s): The aim of this study was to develop and evaluate the activity of bispecific antibodies (bsAbs) to enhance natural killer (NK) cell antibody-dependent cellular cytotoxicity (ADCC) against HIV-infected cells.

Design: These bsAbs are based on patient-derived antibodies targeting the conserved gp41 stump of HIV Env, and also incorporate a high-affinity single chain variable fragment (scFv) targeting the activating receptor CD16 on NK cells. Overall, we expect the bsAbs to provide increased affinity and avidity over their corresponding mAbs, allowing for improved ADCC activity against Env-expressing target cells.

Methods: bsAbs and their corresponding mAbs were expressed in 293T cells and purified. The binding of bsAbs and mAbs to their intended targets was determined using Bio-Layer Interferometry, as well as flow cytometry based binding assays on in-vitro infected cells. The ability of these bsAbs to improve NK cell activity against HIV-infected cells was tested using in-vitro co-culture assays, using flow cytometry and calcein release to analyse NK cell degranulation and target cell killing, respectively.

Results: The bsAbs-bound gp41 with similar affinity to their corresponding mAbs had increased affinity for CD16. The bsAbs also bound to primary $CD4^+$ T cells infected *in vitro* with two different strains of HIV. In addition, the bsAbs induce increased NK cell degranulation and killing of autologous HIV-infected $CD4^+$ T cells.

Conclusion: On the basis of their in-vitro killing efficacy, bsAbs may provide a promising strategy to improve NK-mediated immune targeting of infected cells during HIV infection.

AIDS 2020, **34**:1313–1323

Keywords: antibody-dependent cellular cytotoxicity, bispecific antibody, gp41, HIV, natural killer cells

Introduction

Natural killer (NK) cells are effector cells of the innate immune system that are equipped to recognize and rapidly eradicate tumour or virus-infected cells. Healthy cells escape NK cell killing because major histocompatibility complex class I (MHC-I) proteins on healthy cells engage NK cell inhibitory receptors [1]. In the context of HIV infection, downregulation of MHC-I proteins can activate NK cells; in addition, upregulation of stress-induced ligands on infected cells can trigger engagement of activating receptors on NK

[a]Department of Biochemistry, [b]Department of Medicine, Division of Infectious Diseases and Geographic Medicine, [c]Program in Immunology, School of Medicine, Stanford University, Stanford, California, [d]Department of Biostatistics, University of Washington, Seattle, Washington, [e]Chan Zuckerberg Biohub, San Francisco, and [f]Stanford ChEM-H, Stanford University, Stanford, California, USA.

Correspondence to Catherine A. Blish, MD, PhD, Division of Infectious Diseases and Geographic Medicine, 300 Pasteur Dr, Lane Building, L-134, Stanford, CA 94305, USA.

E-mail: cblish@stanford.edu

[*] Nitya S. Ramadoss and Nancy Q. Zhao contributed equally to this work.

Received: 9 September 2019; revised: 2 March 2020; accepted: 5 March 2020.

DOI:10.1097/QAD.0000000000002543

ISSN 0269-9370

cells such as NKG2D [2]. However, HIV possesses mechanisms to counteract NK cell surveillance, such as downregulation of activating ligands [3,4]. Thus, although NK cells have the potential to control HIV, enhancing their responses could optimize their ability to control HIV.

NK cell effector function can also be antibody-dependent, a process termed antibody-dependent cellular cytotoxicity (ADCC). NK cells expressing the activating cell surface receptor Fc?RIIIA (CD16) can bind antibodies via their constant (Fc) domain; these antibodies can in turn bind cell surface viral antigens. CD16-antibody binding activates NK cells, triggering the secretion of antiviral cytokines such as interferon-gamma (IFN-γ) and the release of perforin and granzymes into target cells, resulting in cell death. ADCC may provide a protective or therapeutic benefit in HIV infection; ADCC antibody titres inversely correlate with viral load and rate of disease progression in HIV-infected individuals [5,6], and are higher in elite controllers than in patients that progress to disease [7]. Furthermore, in mother–infant transmission of HIV, ADCC antibodies in breast milk correlate with reduced infection risk in infants via breastfeeding, while increasing survival rates in infected infants [8,9]. In nonhuman primates, vaccine-induced ADCC antibody titres correlate with decreased viral loads and/or delayed disease progression after challenge with simian immunodeficiency virus (SIV) [10,11]. In humans, the RV144 clinical trial, which was the first HIV vaccine trial to demonstrate some degree of efficacy [12], induced ADCC responses in vaccine recipients [13,14]. Binding of IgGs to V1V2 of Env correlated inversely with the rate of infection, suggesting that ADCC-mediating antibodies could have contributed to the observed protection [15]. However, despite the evidence for the protective role of ADCC responses against HIV, it remains unclear whether the key driver of ADCC efficacy in infection is the binding to viral targets, the triggering of effector cell activation or both.

Investigation into the epitopes of ADCC-mediating mAbs in HIV have revealed multiple viral targets, including Env, Gag, Pol, Vpu and Nef [16–20]. Within Env, many ADCC-mediating mAbs target gp120 [21]. Recently, however, a larger number of gp41-targeting mAbs that mediate ADCC have also been characterized [22,23]. During viral membrane fusion, gp120 is shed, and gp41 undergoes a series of conformational changes that exposes various targetable epitopes such as the fusion peptide, the loop region that connects the two heptad regions and the membrane proximal region [24]. The postfusion state of gp41, a six-helix bundle [25–28], remains exposed at the cell surface after viral and host membranes fuse and is often referred to as a stump [29]. How long stumps remain on the surface of infected cells postfusion has been poorly studied; however, there are some data to suggest that they can remain on the cell surface for at least an hour (longer time points were not tested in this study) [30]. Stumps can also occur on cell surfaces, as gp120 can be shed when virus buds from infected cells [29]. The cell-surface exposed nature of the stumps make them targetable by antigp41, ADCC-mediating mAbs. However, unlike influenza or dengue virions that are densely studded with their envelope glycoproteins, HIV is sparsely coated with Env [31,32]. This presumably results in very few targetable stumps per cell on the surfaces of infected cells, decreasing the overall efficacy of ADCC.

By engineering known antistump, ADCC-mediating mAbs into bispecific antibodies (bsAbs) that adopt a tetravalent IgG-scFv format [33], we rationalized that we would achieve the following. First, we would bridge NK cells to HIV-infected targets via CD16, a potent trigger of NK cell activation [34], thus forcing NK cells to contact and be activated specifically against these cells. Second, the bsAb would show increased avidity over a mAb due to its ability to simultaneously engage two CD16 receptors on the NK cell surface. The resulting increase in local concentration of bsAb at the NK cell surface can enable more efficient crosslinking to the stumps on the infected cell surface. As such, we tested these bsAbs for their ability to activate NK cells and clear HIV-infected primary $CD4^+$ T cells *in vitro*.

Materials and methods

Expression of bispecific antibodies and mAbs

mAbs heavy and light chain plasmids were obtained from Dr Julie Overbaugh (Fred Hutchinson Cancer Research Center). For the bsAbs, the variable heavy chain sequence connected to the NM3E2 scFv sequence via the linker LES(GGGGS)3 (IDT gBlocks) were cloned the VRC01 plasmid backbone (retaining the plasmid's signal sequence and constant heavy chain regions) by In-Fusion. Light chain plasmids from the Overbaugh lab were used as is for bsAb expression. NM3E2 scFv was expressed and purified from *Escherichia coli* as described previously [35].

bsAbs and mAbs were expressed in Expi293 cells, a well established cell line for the production of recombinant antibodies [36,37], at a 2 : 1 Heavy:Light chain ratio, tracking viability (until < 70%) or until day 6, whichever was sooner. Media was harvested and filtered, before purifying bsAbs and mAbs on Protein A columns, followed by size exclusion chromatography (S200 pg or S200 increase for 5 ml or 500 μl scale purification, respectively; GE Healthcare, Chicago, Illinois, USA). All proteins were analysed by reducing and nonreducing SDS-PAGE.

Antigens for biolayer interferometry

Six-helix containing a cysteine in the first HR2 helix (Ser68→Cys68) was expressed and purified as described

previously [38]. The protein was reduced with immobilized TCEP resin (Pierce, Waltham, Massachusetts, USA) using manufacturer's protocols, and conjugated to EZ-Link Maleimide-PEG11-Biotin (Thermo Fisher, Waltham, Massachusetts, USA). The extent of biotinylation was confirmed by HABA assay (Pierce). Excess biotin was removed by washing 10x with 10K Amicon Ultra-0.5 ml centrifugal filters (Millipore, Burlington, Massachusetts, USA, cat. no UFC501096). Commercial sources were used to obtain biotinylated CD16 (ACRO-Biosystems, Newark, Delaware, USA) and the biotinylated 19-mer adjacent loop peptides that overlap by 16 amino acids (Sigma, St Louis, Missouri, USA). Loop peptide 1 is KDQQLLGIWGCSGKLICTT and loop peptide 2 is QLLGIWGCSGKLICTTAVP.

Binding assays by biolayer interferometry

BLI is a label-free optical analytical technique used to measure biomolecular interactions, based on interference patterns of white light reflected from a biosensor tip. Samples in assay buffer (1x TBS + 0.5% BSA) were dispensed into 96-well black flat-bottom plates (Greiner Bio-One, Kremsmünster, Austria) at a volume of 180–200 μl per well; all measurements were performed on the Octet Red96 (Pall ForteBio, Menlo Park, California, USA) at room temperature at 1000 rpm agitation. Streptavidin-coated biosensor tips (Pall ForteBio) were used to capture biotinylated antigens, and typical immobilization levels captured on the AMC sensors varied up to 0.5 nm. Antigen loading was carried out for 30 s, followed by regeneration to remove nonspecifically bound antigen. After two baseline steps of 20 s each, association was performed for 60 s in wells containing antibody dilutions, followed by dissociation in assay buffer for 90 s. Between each antibody sample, a regeneration step was included to eliminate carryover. Raw data were exported and fitted using Prism's (GraphPad Software, San Diego, California, USA) association then dissociation function.

Binding assays by flow cytometry

CHO-WT was obtained through the NIH AIDS Reagent Program, from Dr Carol Weiss and Dr Judith White. These cells express HIV-1 HXB2 gp120 envelope glycoprotein on their surface, are highly fusogenic and readily form syncytia with human $CD4^+$ cells [39]. Cells were plated at 10^5 cells/well in a 96-well flat-bottomed plate (Corning, New York, USA). After 24 h, supernatant media was removed and replaced with FACS buffer. Cells were stained with 1 : 100 dilution of each antibody for 1 h at 4°C, washed, and stained with Alexa 647-conjugated antihuman IgG (H+L) antibody (Thermo Fisher) for 1 h at 4°C. Cells were further washed, dissociated from the plate using TrypLE Express (Gibco) and analysed by flow cytometry on the Accuri C6 (BD Biosciences, San Jose, California, USA).

For binding studies on HIV-1-infected primary human $CD4^+$ T cells, $CD4^+$ T cells were isolated from healthy human donor PBMCs by negative selection with the $CD4^+$ T cell Isolation Kit (Miltenyi Biotec, Bergisch Gladbach, Germany), and activated with plate-bound anti-CD3 (clone OKT3; eBioscience, San Diego, California, USA), anti-CD28/CD49d (BD Biosciences) and PHA-L (eBioscience). After 48 h, $CD4^+$ T cells were mock-infected, or infected with either Q23 [40] or NL4–3 (infectious molecular clone obtained through the NIH AIDS Reagent Program, from Dr Malcom Martin [41]) virus, using Viromag magnetofection (OZ Biosciences, San Diego, California, USA). Both Q23 and NL4–3 viruses were grown in 293T cells and titrated as previously described [42]. Twenty-four hours post infection, cells were stained at a 10 nmol/l concentration of each mAb/bsAb for 30 min at 4°C, washed, and then stained with Alexa 647-conjugated antihuman IgG (H+L) antibody (Thermo Fisher) for 30 min at 4°C. Cells were further washed, fixed with FACS Lyse (BD Biosciences) and permeabilized with FACS Permeabilization Buffer 2 (BD Biosciences), stained for HIV p24 (KC57-FITC; Beckman Coulter) and analysed by flow cytometry on a MACSQuant Analyzer (Miltenyi Biotec).

Natural killer-$CD4^+$ co-culture assays

NK cells and $CD4^+$ T cells were isolated from donor PBMCs using the NK Cell Isolation Kit and the CD4+ T cell Isolation Kit respectively (Miltenyi Biotec). NK cells were activated for 72 h in 300 IU/ml rhIL-2 (R&D Systems, Minneapolis, Minnesota, USA). $CD4^+$ T cells were simultaneously activated and infected as described above. NK cells were co-cultured with the infected or uninfected $CD4^+$ T cells at a 1 : 1 effector:target (E:T) ratio for 4 h, either in the absence of or with increasing concentrations of bsAb or mAb. NK cells were identified by staining for CD3-V450 and CD56-PE-Cy7; their activation was monitored by staining for CD107a-APC (all antibodies from Biolegend). Cells were analysed by flow cytometry on a MACSQuant Analyzer (Miltenyi Biotec). All flow cytometry analysis was performed using FlowJo version 9.9.6 (Tree Star, Ashland, Oregon, USA).

For cytotoxicity assays, target $CD4^+$ T cells were loaded with 2.5 μmol/l calcein-AM (Invitrogen), and incubated with autologous IL-2 activated NK cells at a 4 : 1 E:T ratio [43]. After a 4 h incubation, cells were spun down and 100 μl of culture supernatant was transferred into 96-well black flat-bottom plates (Greiner Bio-One), and calcein release into the supernatant was measured using a Synergy HTX fluorescent plate reader (Biotek, Winooski, Vermont, USA), with control wells containing no effector cells (spontaneous lysis) and with 2% Tween-20 (maximum lysis). Specific killing was calculated using the equation: specific killing = (effector lysis - spontaneous lysis)/(maximum lysis - spontaneous lysis) x 100%.

Statistical analysis

For co-culture assays, linear mixed effects models were used. The models incorporated fixed effects for

concentration, bsAb vs. mAb, and mock vs. HIV infection, and a random effect for donor. This model takes into account that there are multiple observations per donor and accounts for variability between donors. Statistical analyses were performed using SPSS and the *nlme* package in R (R Foundation, Vienna, Austria).

Results

Expression and purification of stump-targeting bispecific antibodies

To improve ADCC activity of stump-targeting mAbs, we designed bsAbs in the IgG-scFv or Morrison format [33,44], in which the variable regions of the antibody target gp41 stumps on HIV-infected cells, while the high-affinity scFvs tethered to the heavy chains bind CD16 on NK cells. These bsAbs can engage two CD16 receptors on the NK cell while binding to the target antigen, resulting in increased avidity. We chose the IgG-scFv format to retain full Fc effector function on the bsAb, so that we could directly compare bsAb activity to the corresponding mAb. We postulated that the combination of high affinity and avidity would drive high efficacy of the bsAbs compared with the mAbs, which have lower efficacy due to low-affinity Fcs engaging one CD16 on the NK cell surface at a time (Fig. 1a).

For the stump binding antibodies, we used previously identified patient-derived antistump antibodies, QA255.006 and QA255.072, referred to hereafter as 006 and 072, respectively [23]. The 006 antibody binds gp41 stumps and as a stump mimetic, six-helix [23]. The 006 epitope has not been precisely mapped, but is thought to be a discontinuous epitope that includes parts of the C-heptad repeat and N-heptad repeat regions of gp41, and potentially the fusion proximal peptide region (FPPR) of gp41 [23]. The 072 antibody binds a highly conserved linear epitope in the loop region of gp41 [23]. This linear epitope overlaps with the binding epitope of another patient-derived mAb 7B2 [45], as well as other known loop binding mAbs [46,47]. The stump-binding antibodies demonstrate cross-clade binding to HIV-1 strains. For the CD16-targeting scFv portion of the bsAbs, we used NM3E2, a phage-display derived antibody [35]. After expression in mammalian cells, bsAbs and mAbs were isolated using Protein A resin, followed by size exclusion chromatography. As expected, the bsAbs eluted earlier than the mAbs on the size exclusion column due to their larger molecular weights (Fig. 1c, Supplemental Fig 1, http://links.lww.com/QAD/B711).

bispecific antibodies show increased affinity to CD16 over mAbs, while engaging stumps with similar affinity

To determine whether bsAbs showed improved binding to CD16 over mAbs, we used biolayer interferometry (BLI), and compared binding of the bsAbs, mAbs and the NM3E2 scFv with CD16. The bsAbs demonstrated binding in the nanomolar range to CD16, which were two to three orders of magnitude improved over that of the mAbs (low to sub-micromolar range) (Fig. 2a, Table 1). NM3E2 scFv affinity was determined to be 75.1 ± 15.1 nmol/l, which is within an order of magnitude of the published value of 20 nmol/l for this scFv [35].

To determine whether bsAbs retained their binding specificities and affinities to their targets, we used BLI and compared binding of the bsAbs, mAbs and NM3E2 with six-helix, the stump mimetic that has been shown to be targeted by 006 but not 072 (as six-helix does not contain the immunodominant loop that 072 binds to), as well as two 19-mer loop peptides that both contain the previously determined linear epitope of 072 [23], but that do not bind 006. Recombinantly expressed gp41 ectodomain was insoluble in the BLI assay buffer, and therefore not used in this assay. bsAbs and IgGs demonstrated similar levels of binding (Table 1), and retained their binding specificities to their corresponding targets, that is, 006 bsAb and IgG bound six-helix but not loop peptides, while 072 bsAb and IgG-bound loop peptides but not 006 (Fig. 2b, c).

Bispecific antibodies bind to cells expressing Env, as well as to HIV-infected primary $CD4^+$ T cells

The stump-binding mAbs have previously been shown to bind to Env in a cell-based ELISA assay [23]. To determine whether the constructs could engage their targets on the surface of cells, we first tested binding of the mAbs and bsAbs in adherent CHO cells expressing HXB2 gp120. mAbs and bsAbs bind 9–12% of Env-expressing CHO cells, six to seven-fold greater than the background secondary only control (Fig. 3a). These results correlate with the binding of bsAbs and mAbs *in vitro*, showing that in the absence of NK cells or CD16, binding profiles of the bsAbs and mAbs to the target antigen are similar. We then tested dose-dependence of cell-surface binding with the 006 and 072 mAbs. Binding to Env-expressing CHO cells was dose-dependent for both 006 and 072 in the 0–500 nmol/l range (Supplemental Figure 2A, http://links.lww.com/QAD/B711).

To evaluate binding of these bsAbs to Env in a more physiological system, we tested the binding of the mAbs and bsAbs to primary $CD4^+$ T cells infected *in vitro* with either a clone from early, subtype A infection (Q23) or a commonly used laboratory-adapted, subtype B strain (NL4–3). The Q23 strain was used as the 006 and 072 mAbs were derived from an individual with subtype A infection [23]; the NL4–3 strain was used to test cross-reactivity in a different subtype. To exclude bystander uninfected cells, we only included HIV $p24^+$ cells in the analysis. Both the 072 and 006 bsAbs and mAbs demonstrated binding to HIV-1-infected $CD4^+$ T cells, with 60–80% of infected cells staining positively in Q23-infected cells and 13–40% in NL4–3 infected cells;

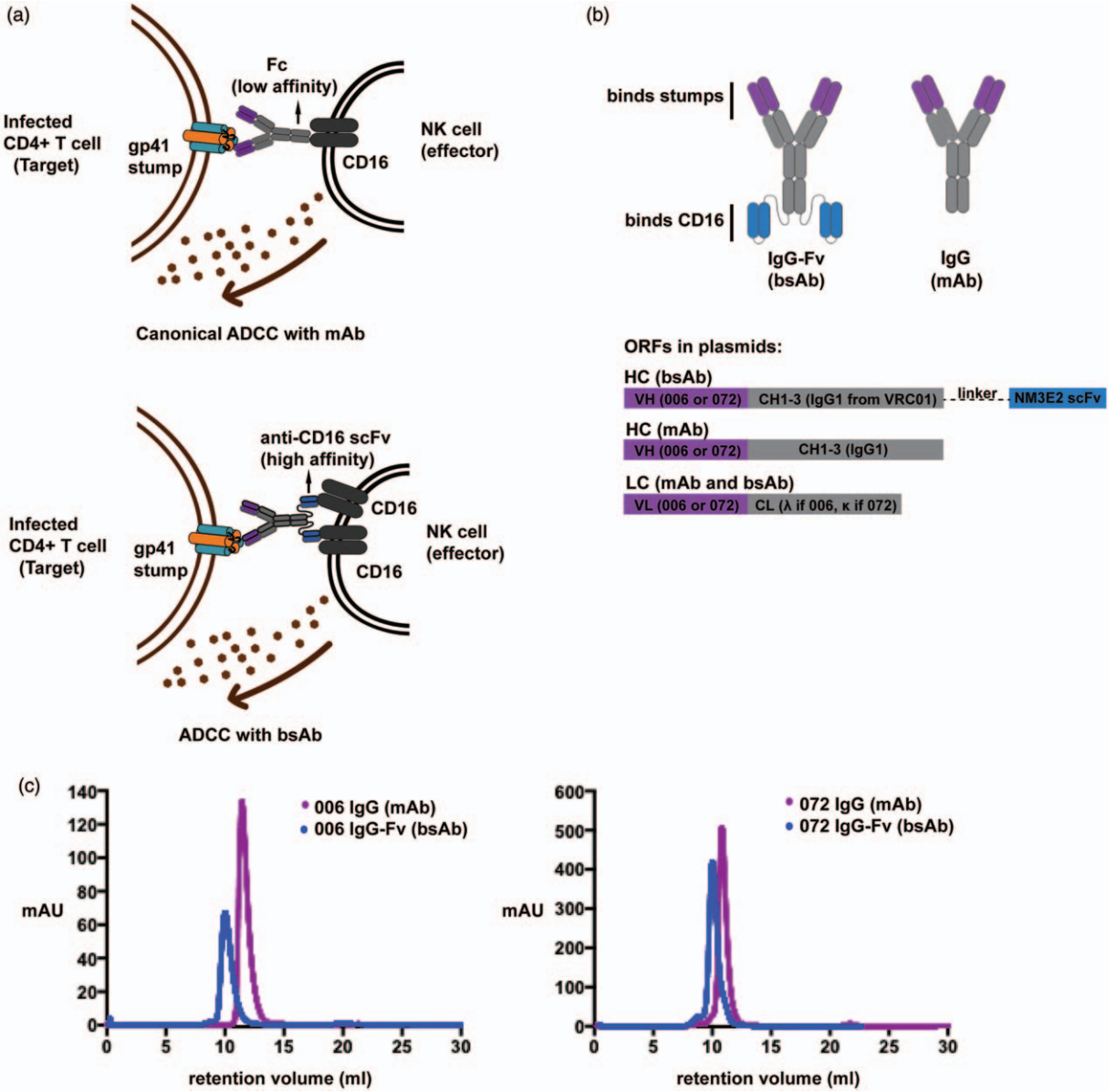

Fig. 1. (a) Schematic describing the difference between canonical ADCC with a mAb (top), and ADCC with a bsAb. A mAb binds to CD16 via its low affinity Fc to drive ADCC. With a bsAb, the high affinity of the scFvs tethered to the heavy chains, together with increased avidity from their binding two CD16 receptors on the NK cell potentially drives higher efficacy. This specific activation of NK cells results in lysis of the infected target via production of cytolytic granules. (b) Schematic describing bsAb and mAb constructs (top) and the ORFs encoding these antibodies in the plasmids used for transfection (bottom). (c) IgG-Fv bispecific antibodies (bsAbs) and corresponding stump-binding mAbs were expressed in Expi293 cells, and purified by size exclusion chromatography on an S200 column after an initial protein A purification step. IgG-Fvs (~200 kD, blue) elute earlier than IgGs (~150 kDa, purple) as expected.

binding was similar between bsAbs and mAbs (Fig. 3c). No binding higher than 1% was observed for either bsAb or mAb to mock-infected cells (Supplemental Figure 2B, http://links.lww.com/QAD/B711).

Bispecific antibodies improve natural killer cell mediated killing of autologous HIV-infected cells

To determine if the bsAbs could improve NK cell targeting of autologous HIV-1-infected cells, we used an in-vitro NK-$CD4^+$ co-culture assay to test the effect of the bsAbs on NK cell degranulation and target cell killing. The range of concentrations tested, from 0.1 to 10 nmol/l, was chosen to be within the testing concentrations previously documented [35]. NK cell degranulation significantly increased, in co-culture with $CD4^+$ T cells infected with either the Q23 or NL4–3 strains, in the presence of increasing concentrations of the bsAb (Fig. 4a). A similar increase was not observed with

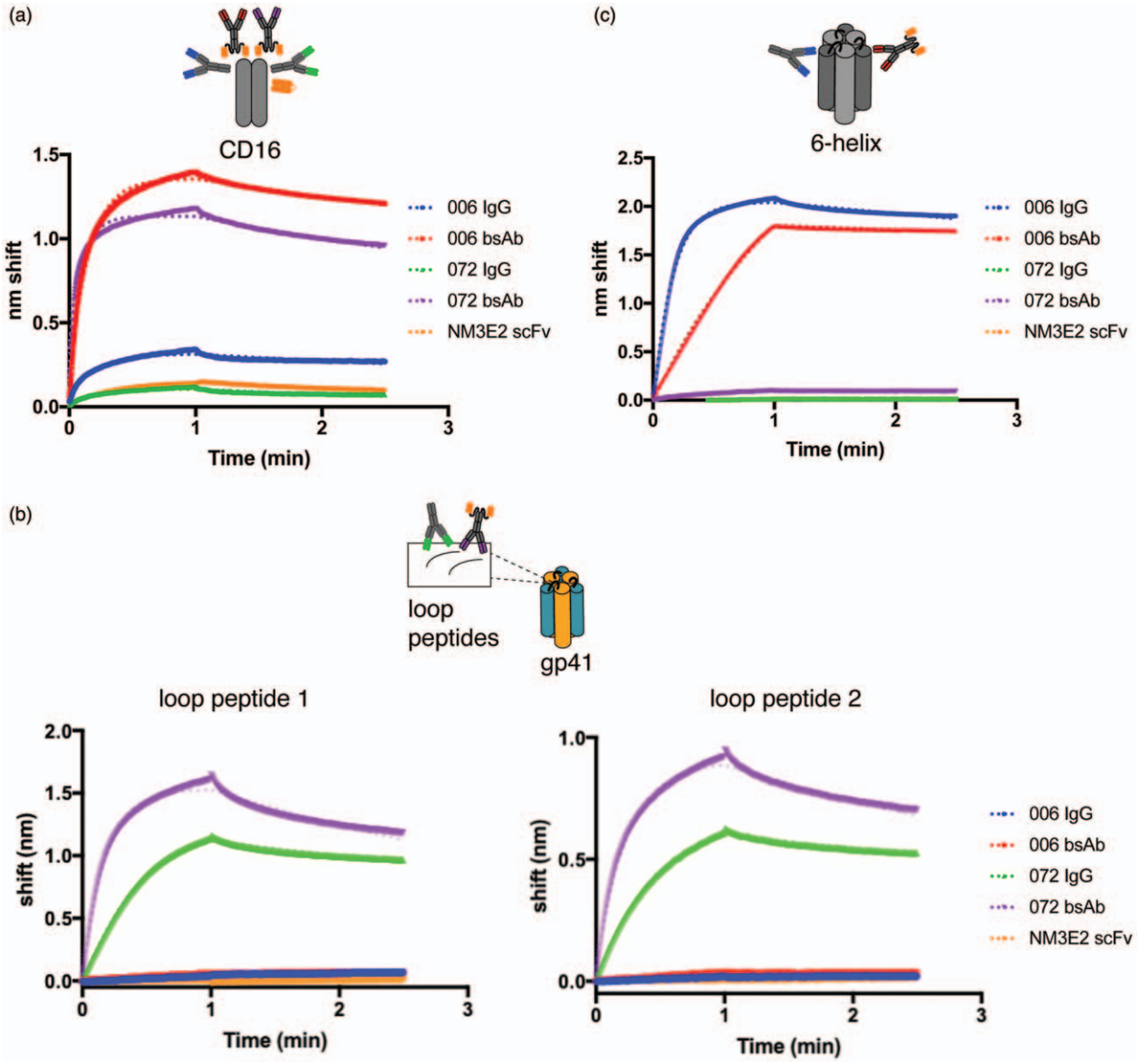

Fig. 2. Binding of mAbs and bsAbs to (a) CD16, (b) loop peptides 1 and 2 containing 072 epitope and (c) 6-helix as determined by Bio-layer Interferometry. Representative curves from 3 biological repeats shown. Fits are indicated in the dotted lines. Cartoon insets above each graph indicate the binding target tested in each case and the antibodies that are expected to bind.

mock-infected cells. We also tested the 072 and 006 mAbs in the same assay, to determine if the bsAbs' enhanced affinity and avidity improved NK cell targeting compared with the corresponding mAbs. As expected, the 072 and 006 bsAbs induced much stronger NK cell degranulation responses than the mAbs - at 10 nmol/l, NK degranulation was between 2.5 and 3.5-fold higher in the presence of the bsAbs than their matched mAbs (Fig. 4a). For each of the 072 and 006 constructs, we used a linear mixed model [48], with a random effect for donor to

Table 1. Apparent binding constants (Kapp)[a] of Abs to six-helix, loop peptides and CD16.

	006 IgG	006 IgG-Fv	072 IgG	072 IgG-Fv	NM3E2 scFv
CD16	0.37 ± 0.26 μmol/l	4.6 ± 2.4 nmol/l	4.9 ± 4.4 μmol/l	9.7 ± 6.1 nmol/l	72 ± 14 nmol/l
Six-helix	2.5 ± 0.55 nmol/l	1.6 ± 0.20 nmol/l	No binding	No binding	No binding
Loop peptide 1	No binding	No binding	3.2 ± 1.1 nmol/l	2.5 ± 0.67 nmol/l	No binding
Loop peptide 2	No binding	No binding	3.1 ± 1.4 nmol/l	6.4 ± 3.9 nmol/l	No binding

[a]Values reported as mean ± SD for three biological repeats.

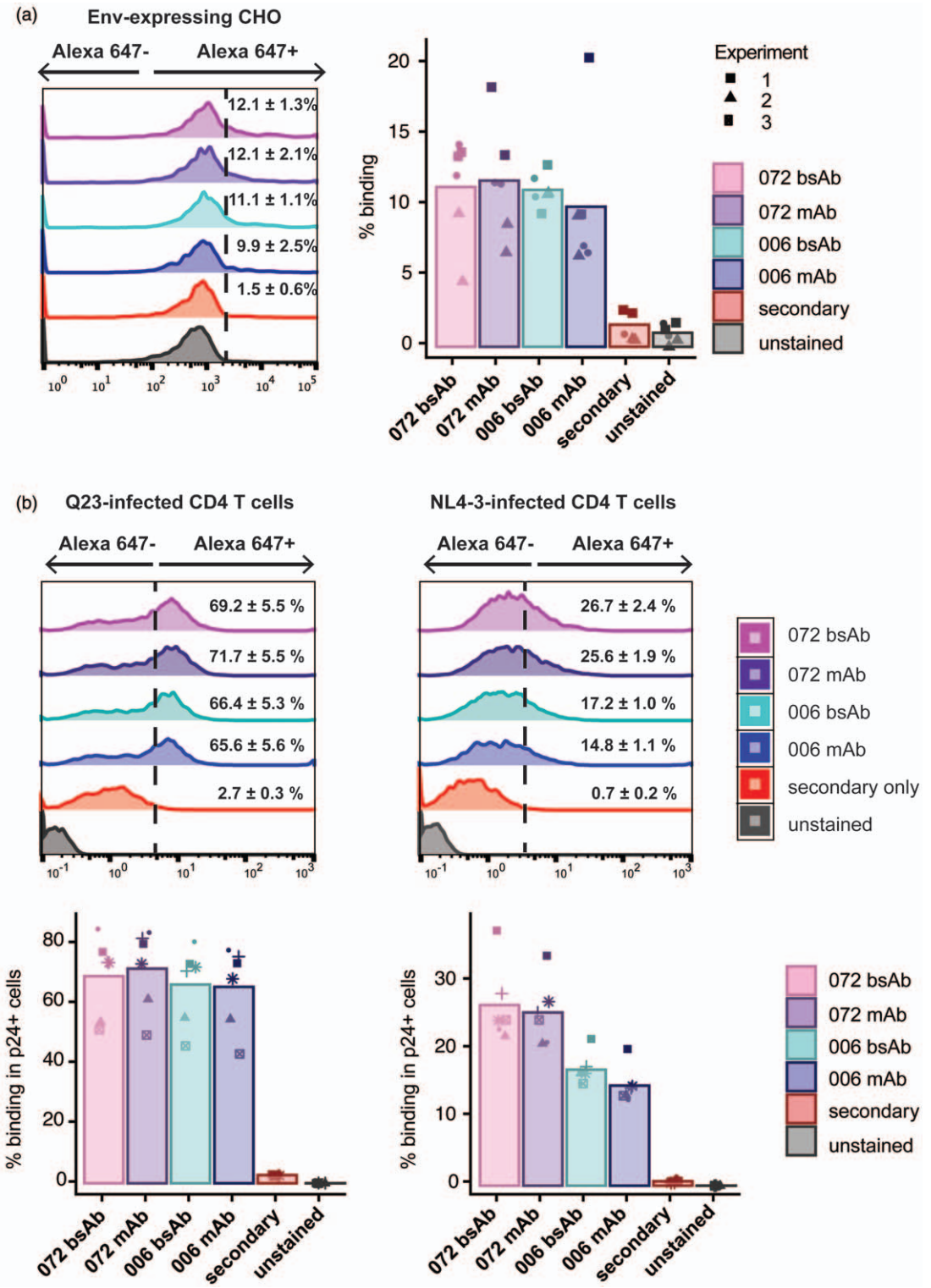

Fig. 3. Binding of antibodies (bsAbs and mAbs) to (a) CHO-WT cells expressing Env and (b) primary CD4$^+$ T cells infected *in vitro* with either a clone from early subtype A HIV infection (Q23) or laboratory-adapted (NL4–3) strain of HIV. For each, histograms of antibody binding are shown for one representative repeat; the dotted line indicates the gate set based on the secondary only stained control. Mean percentage positive binding and corresponding SEM are shown numerically for each antibody. In the bar graph, percentage positive binding of each antibody is shown for each of (a) three separate biological repeats, each with two replicates and (b) six biological replicates, and mean values for each antibody are shown in the overlaid bar graph. Shapes denote individual biological replicates.

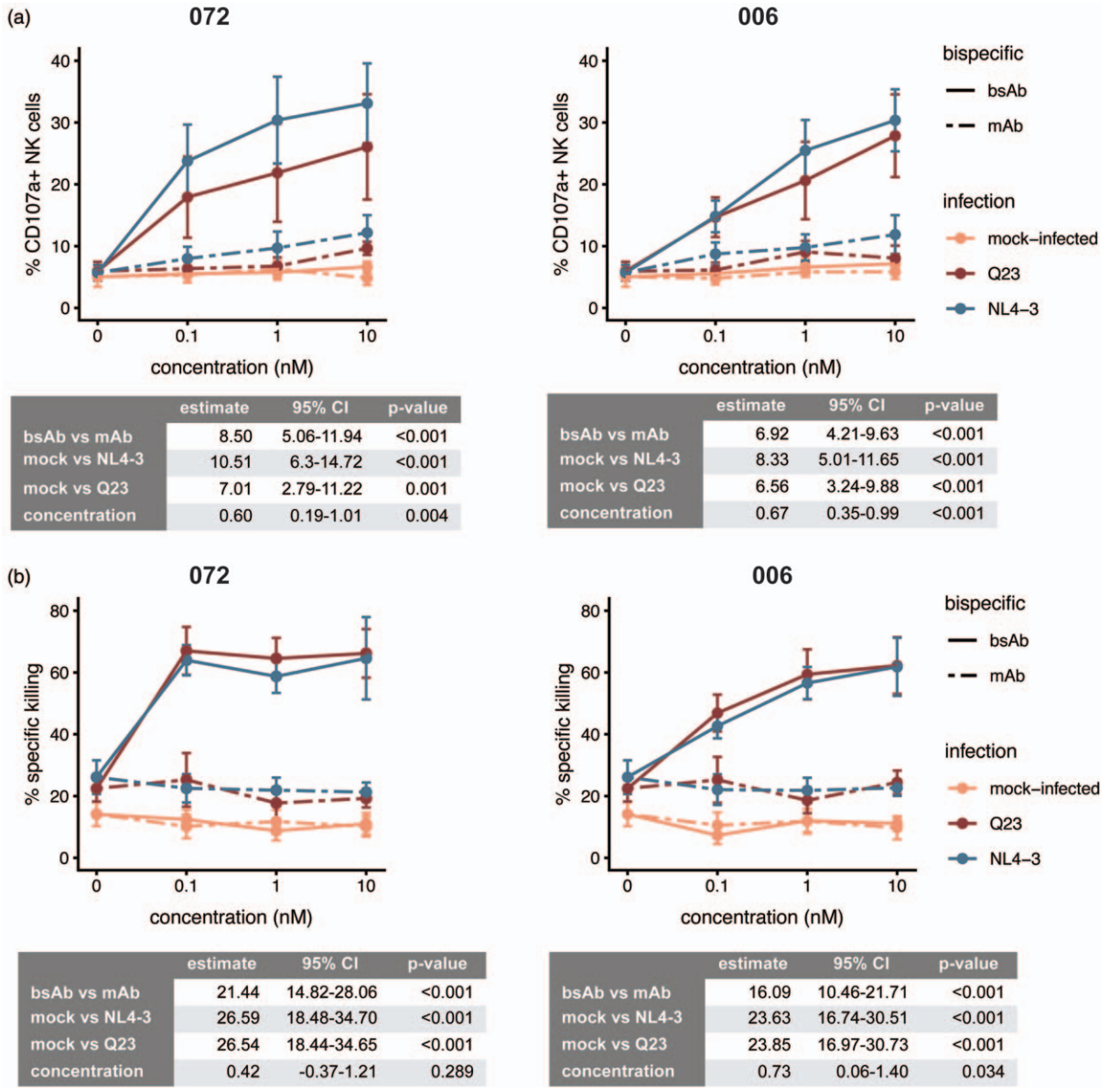

	estimate	95% CI	p-value
bsAb vs mAb	8.50	5.06-11.94	<0.001
mock vs NL4-3	10.51	6.3-14.72	<0.001
mock vs Q23	7.01	2.79-11.22	0.001
concentration	0.60	0.19-1.01	0.004

	estimate	95% CI	p-value
bsAb vs mAb	6.92	4.21-9.63	<0.001
mock vs NL4-3	8.33	5.01-11.65	<0.001
mock vs Q23	6.56	3.24-9.88	<0.001
concentration	0.67	0.35-0.99	<0.001

	estimate	95% CI	p-value
bsAb vs mAb	21.44	14.82-28.06	<0.001
mock vs NL4-3	26.59	18.48-34.70	<0.001
mock vs Q23	26.54	18.44-34.65	<0.001
concentration	0.42	-0.37-1.21	0.289

	estimate	95% CI	p-value
bsAb vs mAb	16.09	10.46-21.71	<0.001
mock vs NL4-3	23.63	16.74-30.51	<0.001
mock vs Q23	23.85	16.97-30.73	<0.001
concentration	0.73	0.06-1.40	0.034

Fig. 4. Natural killer cell responses to autologous primary CD4$^+$ T cells that were mock-infected (orange) or infected with either an early subtype A clone (Q23, red) or a laboratory-adapted, subtype B strain (NL4–3, blue) of HIV, in the presence of varying concentrations of the bsAbs/mAbs, were assessed by (a) degranulation of NK cells as measured by % positive for CD107a by FACS, and (b) killing, as detected by calcein release. The data represent the mean and SEM for six (a) and four (b) donors, respectively. Estimates for the contribution of each of the factors tested to % CD107a+ (a) or % specific killing (b) in the linear mixed model are shown in the table below each figure, together with 95% confidence intervals and *P* value.

account for inter-individual variability, to test the contributions of concentration, HIV infection and bsAb/mAb on NK cell degranulation. In the model, concentration, infection (with either strain of HIV-1) and bsAb (vs. mAb) were all found to have a statistically significant effect on NK cell degranulation, for both bsAbs.

To determine whether the increases in NK cell degranulation also led to increased killing of HIV-1-infected target cells, we measured target cell death using calcein release [43]. Both bsAbs significantly enhanced NK killing of HIV-infected cells with increasing concentration, for both strains of HIV-1 tested, and had little nonspecific targeting, as killing of mock-infected cells was not increased (Fig. 4b). Once again, the 072 and 006 bsAbs induced higher levels of target cell death in the presence of NK cells compared with their corresponding mAbs at matched concentrations (Fig. 4b). In linear mixed models, infection (with either strain of HIV) and bsAb (vs mAb) were both found to have a statistically significant effect on NK cell degranulation;

concentration had a statistically significant effect on the 006 bsAb but not the 072. The bsAb format enabled improved NK cell targeting and killing of infected cells over the mAb; this improved targeting was HIV-specific, and was observed across two HIV-1 strains of different subtypes.

Discussion

NK cells can rapidly recognize and lyse virus-infected or malignant cells; however, cancers and viruses have developed strategies to avoid NK cell surveillance. Thus, there is a need to specifically activate NK cells to overcome these evasion strategies. bsAbs have previously been used successfully in the cancer setting to enhance NK cell activity and clear tumours such as non-Hodgkin's lymphoma [49] and acute myeloid leukaemia [50]. In contrast, little work has been done in the field of bsAbs to recruit NK cells to treat viral infections. This work shows that NK cell activity against HIV-1 can be specifically enhanced using bsAbs that simultaneously target gp41 on HIV-infected cells and the activating receptor CD16 on NK cells. As CD16 is expressed on other effector cell types such as macrophages and neutrophils [51,52], activation of non-NK cells might be a concern; however, even if this were to occur, these effectors would likely augment the clearance of infected cells. In addition, effector cells can express phenotypic variants of the CD16 receptor. To this end, we tested binding of our bsAbs to two CD16a variants using ELISAs and found that the binding remained unchanged between the two variants (Supplemental Fig 3, http://links.lww.com/QAD/B711).

Recently, one study has linked single domain soluble CD4 to an anti-CD16 antibody to exploit the high-affinity interaction between gp120 and its native receptor CD4 [53]. Soluble CD4 confers broad-spectrum recognition of envelope glycoprotein across different HIV strains. However, a potential limitation of this strategy is that CD4 can induce gp120 shedding, which can decrease binding over time. Our alternative approach of targeting gp41 avoids this limitation. Another abstract described NK cell activation in the context of HIV by linking a known gp120-binding broadly neutralizing antibody, VRC01 to an anti-CD16 single chain nanobody [54]. Our study differs from this aforementioned work as a proof of principle to determine the feasibility of using tetravalent bsAbs to enhance NK cell function against HIV, particularly by using gp41 antibodies to target infected cells. Presumably, this strategy can be extended to enhancing NK cell function in other disease contexts, such as influenza, wherein ADCC responses are also known to be protective [55].

The gp41 antibodies used in the bsAb constructs in this study were recently shown in a separate study to mediate ADCC in the commonly used RF-ADCC assay that employs cells coated with HIV Env [23]. In the context of in-vitro infected cells, the binding of these mAbs was much lower (Fig. 3b), which is unsurprising given the low density of Env on infected cell surfaces compared with protein-coated cell surfaces. In addition, we observed differences in binding between cells infected with Q23 or NL4–3; this may reflect differences in binding of the gp41 antibodies between Env proteins between the two strains, or differences in the level of expression of Env between the two strains. Binding of the gp41 mAbs was increased when infecting cells with Vpu/Nef-deficient virus (which results in higher Env surface expression), or in a cell-based ELISA wherein soluble CD4 was used to induce gp120 shedding to expose the gp41 epitopes [23]. However, to overcome the reduced ADCC activity due to low binding of the mAbs in in-vitro infected cells, we employed a more therapeutically translatable approach and enhanced ADCC activity by the tetravalent bsAb format to increase affinity and avidity to CD16, compared with the corresponding mAbs. The bsAb platform is an exciting tool to modulate NK cell function, with the potential for improved activity and specificity in future studies. For instance, studies targeting other activating receptors on NK cells, such as NKG2D, are warranted. In addition, two distinct activating receptors on the NK cell can be targeted to engineer a trispecific antibody (two specificities to the NK cell, and one to the infected target) to fine tune NK activation and the magnitude of effector responses. Much of the focus for enhancing ADCC has previously only been on the level of the antibody, either on its Fab affinity to its target, or on its Fc type. Our work emphasizes the importance of improving effector cell activation to boost therapeutic outcomes.

Overall, we have demonstrated that NK cell cytotoxicity against HIV-1 can be specifically enhanced using bsAbs targeting both the gp41 region of HIV Env and the activating receptor CD16 on NK cells, providing a new avenue for immune targeting of HIV infection.

Acknowledgements

We are grateful for the gift of mAb plasmids from Dr Julie Overbaugh at the Fred Hutchinson Cancer Research Center.

N.S.R. and N.Q.Z. designed and performed research, and analysed data. B.A.R. assisted in statistical analyses. P.M.G. contributed samples to the study. P.S.K. and C.A.B. supervised the study. N.S.R., N.Q.Z., P.S.K. and C.A.B. wrote the manuscript, with input from all authors.

This work was supported by NIH DP1 DA04508902 (C.A.B.), Bill & Melinda Gates Foundation and Stanford Human Systems Immunology Center Pilot Grant (C.A.B.), Burroughs Wellcome Fund Investigators in the Pathogenesis of Infectious Diseases (C.A.B.), NIH DP1 DA043893 (P.S.K.) and Virginia and Ludwig Fund for Cancer Research (P.S.K.). N.Q.Z. was supported by a National Science Scholarship from the Agency for Science, Technology and Research (A*STAR) Singapore. P.S.K. and C.A.B. are investigators of the Chan Zuckerberg Biohub.

Conflicts of interest

There are no conflicts of interest.

References

1. Pegram HJ, Andrews DM, Smyth MJ, Darcy PK, Kershaw MH. **Activating and inhibitory receptors of natural killer cells.** *Immunol Cell Biol* 2011; **89**:216–224.
2. Richard J, Sindhu S, Pham TNQ, Belzile J-P, Cohen EA. **HIV-1 Vpr up-regulates expression of ligands for the activating NKG2D receptor and promotes NK cell-mediated killing.** *Blood* 2010; **115**:1354–1363.
3. Cerboni C, Neri F, Casartelli N, Zingoni A, Cosman D, Rossi P, *et al*. **Human immunodeficiency virus 1 Nef protein down-modulates the ligands of the activating receptor NKG2D and inhibits natural killer cell-mediated cytotoxicity.** *J Gen Virol* 2007; **88**:242–250.
4. Matusali G, Potesta M, Santoni A, Cerboni C, Doria M. **The human immunodeficiency virus type 1 Nef and Vpu proteins down-regulate the natural killer cell activating ligand PVR.** *J Virol* 2012; **86**:4496–4504.
5. Ahmad R, Sindhu ST, Toma E, Morisset R, Vincelette J, Menezes J, *et al*. **Evidence for a correlation between antibody-dependent cellular cytotoxicity-mediating anti-HIV-1 antibodies and prognostic predictors of HIV infection.** *J Clin Immunol* 2001; **21**:227–233.
6. Baum LL, Cassutt KJ, Knigge K, Khattri R, Margolick J, Rinaldo C, *et al*. **HIV-1 gp120-specific antibody-dependent cell-mediated cytotoxicity correlates with rate of disease progression.** *J Immunol* 1996; **157**:2168–2173.
7. Lambotte O, Ferrari G, Moog C, Yates NL, Liao H-X, Parks RJ, *et al*. **Heterogeneous neutralizing antibody and antibody-dependent cell cytotoxicity responses in HIV-1 elite controllers.** *AIDS* 2009; **23**:897–906.
8. Mabuka J, Nduati R, Odem-Davis K, Peterson D, Overbaugh J. **HIV-specific antibodies capable of ADCC are common in breastmilk and are associated with reduced risk of transmission in women with high viral loads.** *PLoS Pathog* 2012; **8**:e1002739.
9. Milligan C, Richardson BA, John-Stewart G, Nduati R, Overbaugh J. **Passively acquired antibody-dependent cellular cytotoxicity (ADCC) activity in HIV-infected infants is associated with reduced mortality.** *Cell Host Microbe* 2015; **17**:500–506.
10. Barouch DH, Liu J, Li H, Maxfield LF, Abbink P, Lynch DM, *et al*. **Vaccine protection against acquisition of neutralization-resistant SIV challenges in rhesus monkeys.** *Nature* 2012; **482**:89–93.
11. Gómez-Román VR, Patterson LJ, Venzon D, Liewehr D, Aldrich K, Florese R, *et al*. **Vaccine-elicited antibodies mediate antibody-dependent cellular cytotoxicity correlated with significantly reduced acute viremia in rhesus macaques challenged with SIVmac251.** *J Immunol* 2005; **174**:2185–2189.
12. Rerks-Ngarm S, Pitisuttithum P, Nitayaphan S, Kaewkungwal J, Chiu J, Paris R, *et al*. **Vaccination with ALVAC and AIDSVAX to prevent HIV-1 infection in Thailand.** *N Engl J Med* 2009; **361**:2209–2220.
13. Karnasuta C, Paris RM, Cox JH, Nitayaphan S, Pitisuttithum P, Thongcharoen P, *et al*. **Antibody-dependent cell-mediated cytotoxic responses in participants enrolled in a phase I/II ALVAC-HIV/AIDSVAX B/E prime-boost HIV-1 vaccine trial in Thailand.** *Vaccine* 2005; **23**:2522–2529.
14. Bonsignori M, Pollara J, Moody MA, Alpert MD, Chen X, Hwang K-K, *et al*. **Antibody-dependent cellular cytotoxicity-mediating antibodies from an HIV-1 vaccine efficacy trial target multiple epitopes and preferentially use the VH1 gene family.** *J Virol* 2012; **86**:11521–11532.
15. Haynes BF, Gilbert PB, McElrath MJ, Zolla-Pazner S, Tomaras GD, Alam SM, *et al*. **Immune-correlates analysis of an HIV-1 vaccine efficacy trial.** *N Engl J Med* 2012; **366**:1275–1286.
16. Grunow R, Franke L, Hinkula J, Wahren B, Fenyö EM, Jondal M, *et al*. **Monoclonal antibodies to p24-core protein of HIV-1 mediate ADCC and inhibit virus spread in vitro.** *Clin Diagn Virol* 1995; **3**:221–231.
17. Isitman G, Stratov I, Kent SJ. **Antibody-dependent cellular cytotoxicity and NK cell-driven immune escape in HIV infection: implications for HIV vaccine development.** *Adv Virol* 2012; **2012**:637208.
18. Yamada T, Watanabe N, Nakamura T, Iwamoto A. **Antibody-dependent cellular cytotoxicity via humoral immune epitope of Nef protein expressed on cell surface.** *J Immunol* 2004; **172**:2401–2406.
19. Wren LH, Chung AW, Isitman G, Kelleher AD, Parsons MS, Amin J, *et al*. **Specific antibody-dependent cellular cytotoxicity responses associated with slow progression of HIV infection.** *Immunology* 2013; **138**:116–123.
20. Tiemessen CT, Shalekoff S, Meddows-Taylor S, Schramm DB, Papathanasopoulos MA, Gray GE, *et al*. **Cutting edge: unusual NK cell responses to HIV-1 peptides are associated with protection against maternal-infant transmission of HIV-1.** *J Immunol* 2009; **182**:5914–5918.
21. Pollara J, Bonsignori M, Moody MA, Pazgier M, Haynes BF, Ferrari G. **Epitope specificity of human immunodeficiency virus-1 antibody dependent cellular cytotoxicity [ADCC] responses.** *Curr HIV Res* 2013; **11**:378–387.
22. Yang Z, Liu X, Sun Z, Li J, Tan W, Yu W, *et al*. **Identification of a HIV Gp41-specific human monoclonal antibody with potent antibody-dependent cellular cytotoxicity.** *Front Immunol* 2018; **9**:2613.
23. Williams KL, Stumpf M, Naiman NE, Ding S, Garrett M, Gobillot T, *et al*. **Identification of HIV gp41-specific antibodies that mediate killing of infected cells.** *PLoS Pathog* 2019; **15**:e1007572.
24. Harrison SC. **Mechanism of membrane fusion by viral envelope proteins.** *Adv Virus Res* 2005; **64**:231–261.
25. Chan DC, Fass D, Berger JM, Kim PS. **Core structure of gp41 from the HIV envelope glycoprotein.** *Cell* 1997; **89**:263–273.
26. Weissenhorn W, Dessen A, Harrison SC, Skehel JJ, Wiley DC. **Atomic structure of the ectodomain from HIV-1 gp41.** *Nature* 1997; **387**:426–430.
27. Lu M, Blacklow SC, Kim PS. **A trimeric structural domain of the HIV-1 transmembrane glycoprotein.** *Nat Struct Biol* 1995; **2**:1075–1082.
28. Blacklow SC, Lu M, Kim PS. **A trimeric subdomain of the simian immunodeficiency virus envelope glycoprotein.** *Biochemistry* 1995; **34**:14955–14962.
29. Moore PL, Crooks ET, Porter L, Zhu P, Cayanan CS, Grise H, *et al*. **Nature of nonfunctional envelope proteins on the surface of human immunodeficiency virus type 1.** *J Virol* 2006; **80**:2515–2528.
30. Egan MA, Carruth LM, Rowell JF, Yu X, Siliciano RF. **Human immunodeficiency virus type 1 envelope protein endocytosis mediated by a highly conserved intrinsic internalization signal in the cytoplasmic domain of gp41 is suppressed in the presence of the Pr55gag precursor protein.** *J Virol* 1996; **70**:6547–6556.
31. Zhu P, Chertova E, Bess J Jr, Lifson JD, Arthur LO, Liu J, *et al*. **Electron tomography analysis of envelope glycoprotein trimers on HIV and simian immunodeficiency virus virions.** *Proc Natl Acad Sci U S A* 2003; **100**:15812–15817.
32. Zhu P, Liu J, Bess J Jr, Chertova E, Lifson JD, Grisé H, *et al*. **Distribution and three-dimensional structure of AIDS virus envelope spikes.** *Nature* 2006; **441**:847–852.
33. Coloma MJ, Morrison SL. **Design and production of novel tetravalent bispecific antibodies.** *Nat Biotechnol* 1997; **15**:159–163.

34. Bryceson YT, March ME, Ljunggren H-G, Long EO. **Synergy among receptors on resting NK cells for the activation of natural cytotoxicity and cytokine secretion.** *Blood* 2006; **107**:159–166.
35. McCall AM, Adams GP, Amoroso AR, Nielsen UB, Zhang L, Horak E, *et al*. **Isolation and characterization of an anti-CD16 single-chain Fv fragment and construction of an anti-HER2/neu/anti-CD16 bispecific scFv that triggers CD16-dependent tumor cytolysis.** *Mol Immunol* 1999; **36**:433–445.
36. Kahl M, Settele F, Knick P, Haupts U, Bosse-Doenecke E. **Mabfilin and Fabfilin: new antibody-scaffold fusion formats for multispecific targeting concepts.** *Protein Expr Purif* 2018; **149**:51–65.
37. Davis-Gardner ME, Alfant B, Weber JA, Gardner MR, Farzan M. **A bispecific antibody that simultaneously recognizes the V2- and V3-glycan epitopes of the HIV-1 envelope glycoprotein is broader and more potent than its parental antibodies.** *MBio* 2020; **11**:e03080–19.
38. Root MJ, Kay MS, Kim PS. **Protein design of an HIV-1 entry inhibitor.** *Science* 2001; **291**:884–888.
39. Weiss CD, White JM. **Characterization of stable Chinese hamster ovary cells expressing wild-type, secreted, and glycosylphosphatidylinositol-anchored human immunodeficiency virus type 1 envelope glycoprotein.** *J Virol* 1993; **67**:7060–7066.
40. Poss M, Overbaugh J. **Variants from the diverse virus population identified at seroconversion of a clade A human immunodeficiency virus type 1-infected woman have distinct biological properties.** *J Virol* 1999; **73**:5255–5264.
41. Adachi A, Gendelman HE, Koenig S, Folks T, Willey R, Rabson A, *et al*. **Production of acquired immunodeficiency syndrome-associated retrovirus in human and nonhuman cells transfected with an infectious molecular clone.** *J Virol* 1986; **59**:284–291.
42. Strauss-Albee DM, Fukuyama J, Liang EC, Yao Y, Jarrell JA, Drake AL, *et al*. **Human NK cell repertoire diversity reflects immune experience and correlates with viral susceptibility.** *Sci Transl Med* 2015; **7**:297ra115.
43. Neri S, Mariani E, Meneghetti A, Cattini L, Facchini A. **Calcein-acetyoxymethyl cytotoxicity assay: standardization of a method allowing additional analyses on recovered effector cells and supernatants.** *Clin Diagn Lab Immunol* 2001; **8**:1131–1135.
44. Fitzgerald J, Lugovskoy A. **Rational engineering of antibody therapeutics targeting multiple oncogene pathways.** *MAbs* 2011; **3**:299–309.
45. Santra S, Tomaras GD, Warrier R, Nicely NI, Liao H-X, Pollara J, *et al*. **Human nonneutralizing HIV-1 envelope monoclonal antibodies limit the number of founder viruses during SHIV mucosal infection in rhesus macaques.** *PLoS Pathog* 2015; **11**:e1005042.
46. Xu JY, Gorny MK, Palker T, Karwowska S, Zolla-Pazner S. **Epitope mapping of two immunodominant domains of gp41, the transmembrane protein of human immunodeficiency virus type 1, using ten human monoclonal antibodies.** *J Virol* 1991; **65**:4832–4838.
47. Cavacini LA, Emes CL, Wisnewski AV, Power J, Lewis G, Montefiori D, *et al*. **Functional and molecular characterization of human monoclonal antibody reactive with the immunodominant region of HIV type 1 glycoprotein 41.** *AIDS Res Hum Retroviruses* 1998; **14**:1271–1280.
48. Bolker BM, Brooks ME, Clark CJ, Geange SW, Poulsen JR, Stevens MHH, *et al*. **Generalized linear mixed models: a practical guide for ecology and evolution.** *Trends Ecol Evol* 2009; **24**:127–135.
49. Glorius P, Baerenwaldt A, Kellner C, Staudinger M, Dechant M, Stauch M, *et al*. **The novel tribody [(CD20)2xCD16] efficiently triggers effector cell-mediated lysis of malignant B cells.** *Leukemia* 2012; **27**:190.
50. Singer H, Kellner C, Lanig H, Aigner M, Stockmeyer B, Oduncu F, *et al*. **Effective elimination of acute myeloid leukemic cells by recombinant bispecific antibody derivatives directed against CD33 and CD16.** *J Immunother* 2010; **33**:599–608.
51. Abeles RD, McPhail MJ, Sowter D, Antoniades CG, Vergis N, Manakkat Vijay GK, *et al*. **CD14, CD16 and HLA-DR reliably identifies human monocytes and their subsets in the context of pathologically reduced HLA-DR expression by CD14hi/CD16neg monocytes: expansion of CD14hi/CD16pos and contraction of CD14lo/CD16pos monocytes in acute liver fail.** *Cytometry A* 2012; **81A**:823–834.
52. Perussia B, Ravetch JV. **Fc(RIII (CD16) on human macrophages is a functional product of the Fc(RIII-2 gene.** *Eur J Immunol* 1991; **21**:425–429.
53. Li W, Wu Y, Kong D, Yang H, Wang Y, Shao J, *et al*. **One-domain CD4 fused to human anti-CD16 antibody domain mediates effective killing of HIV-1-infected cells.** *Sci Rep* 2017; **7**:9130.
54. Davis ZB, Lenvik T, Hansen L, Felices M, Cooley S, Vallera D, *et al*. **A novel HIV envelope Bi-specific killer engager enhances natural killer cell mediated ADCC responses against HIV-infected cells.** *Blood* 2016; **128**:2517–12517.
55. Jegaskanda S, Weinfurter JT, Friedrich TC, Kent SJ. **Antibody-dependent cellular cytotoxicity is associated with control of pandemic H1N1 influenza virus infection of macaques.** *J Virol* 2013; **87**:5512–5522.